Witnessing Short- and Long-Range Nonstabilizerness via the Information Lattice

Yuliya Bilinskaya,* Miguel F. Martínez,* Soumi Ghosh, Thomas Klein Kvorning, Claudia Artiaco, and Jens H. Bardarson
Department of Physics, KTH Royal Institute of Technology, 106 91, Stockholm, Sweden

(Received 25 November 2025; revised 29 April 2026; accepted 5 October 2026; published 3 November 2026)

We study nonstabilizerness on the information lattice and demonstrate that noninteger local information directly indicates nonstabilizerness. For states with a clear separation of short- and large-scale information, a noninteger total information at large scales Γ serves as a witness of long-range nonstabilizerness. We propose a folding procedure to separate the global and edge-to-edge contributions to Γ. As an example we show that the ferromagnetic ground state of the spin-1/2 three-state Potts model has long-range nonstabilizerness originating from global correlations, while the paramagnetic ground state has at most short-range nonstabilizerness.

DOI: 10.1103/4t3l-hy7z

Introduction—Quantum information theory offers a unifying lens for understanding quantum states and dynamics [1–9]. In the context of condensed matter, states are often classified in terms of the scaling of the subsystem von Neumann entropy, which is a global measure of the total correlations between a subsystem and its complement. In area-law states [1–4], such as ground states of local gapped Hamiltonians and many-body localized states, correlations are mainly local, meaning that the von Neumann entropy of a subsystem scales with its area. This enables efficient representation of such states via matrix product states [4,10,11]. In contrast, volume-law states [5–7], such as midspectrum eigenstates of ergodic Hamiltonians, have correlations involving an extensive number of degrees of freedom. Furthermore, constant subleading corrections to the area-law scaling serve to characterize states with topological order [12–16].

Quantum states can also be characterized by other quantum information properties such as nonstabilizerness. Stabilizer states are closed under Clifford operations and admit an efficient classical representation [17,18]. Generic condensed matter states require non-Clifford unitaries to be reached from a stabilizer state. Such unitaries are constructed from a universal set realized, for example, by the combination of Clifford and T gates. The deviation of a state from a stabilizer state is known as nonstabilizerness, or magic, and has been quantified by different measures [19–27]. While the concept of nonstabilizerness arose in the context of quantum error correction and fault-tolerant quantum computation [28–31], it has increasing relevance in condensed matter and quantum many-body physics [32–50].

Nonstabilizerness has been interpreted as a measure of quantum-state complexity [38,46,51–54] as it quantifies the distance from the easily representable stabilizer states. Other measures based on the distance from other classes of states that admit efficient representations, such as area-law or fermionic Gaussian states [53,55,56], provide similar yet inequivalent quantifications of complexity. The existence of such different classes raises the requirement of a broader classification. For instance, a comprehensive characterization of quantum states can be obtained by looking at the scale of both correlations and nonstabilizerness.

From the point of view of correlations, the information lattice [57,58] provides a universal characterization of quantum states in terms of local information, which quantifies the total amount of correlations per scale ℓ and spatial location n. The information lattice defines the intrinsic correlation length scales of a state, which do not depend on any specific observable [58]. Within the information lattice, local information behaves as a hydrodynamic quantity: under the application of a local quantum gate information can only flow between nearby lattice points and there exist well-defined information currents [57]. This allows us to comprehensively characterize quantum quench dynamics [59–62] and to perform efficient time evolution of large-scale quantum many-body systems [57,63,64]. As opposed to information, there is no well-defined decomposition indicating where and on what scale nonstabilizerness resides, but there are attempts to evaluate nonlocality of nonstabilizerness [65–70], as well as to divide nonstabilizerness into short- and long-range [71–73]. The latter approach relies on an equivalence relation up to shallow local unitary quantum circuits as is done in

*These authors contributed equally to this work.

Published by the American Physical Society under the terms of the Creative Commons Attribution 4.0 International license. Further distribution of this work must maintain attribution to the author(s) and the published article's title, journal citation, and DOI. Funded by Bibsam.

topological classification [15]. This distinction between short- and long-range nonstabilizerness is not captured by just computing a nonstabilizer monotone, which only gives a measure of the total amount of nonstabilizerness in a quantum state.

In this Letter we show that any noninteger value of local information on the information lattice directly indicates nonstabilizerness in a quantum state. Furthermore, in states where there is a clear separation between short- and large-scale local information (we refer to such states as localized), we use the information lattice to define a witness of long-range nonstabilizerness via the total information at large scales Γ [58]. Through a folding procedure, we define a coarse-grained information lattice that allows us to distinguish whether the long-range nonstabilizerness originates from global or edge-to-edge correlations. We exemplify our approach using the spin-1/2 three-state Potts model and characterize its ground states in the paramagnetic and ferromagnetic phases in terms of their nonstabilizerness. While the paramagnetic ground state has at most short-range nonstabilizerness, the ferromagnetic ground state exhibits long-range nonstabilizerness originating from global correlations.

Stabilizer states and the information lattice—We consider an L-qubit chain with Hilbert space $\mathcal{H} = (\mathbb{C}^2)^{\otimes L}$. We denote by $\mathcal{C}_n^\ell$ the subsystem of $\ell+1$ contiguous sites centered at position n, and refer to ℓ as the scale of $\mathcal{C}_n^\ell$. The information lattice of a state ρ acting on $\mathcal{H}$ is a two-dimensional structure where subsystems are ordered hierarchically in terms of location n and scale ℓ [57,58]. Each site in this structure is uniquely specified by the pair (n,ℓ), where n is the integer for even ℓ and half-integer for odd ℓ, and is associated with the local information i_n^ℓ in subsystem $\mathcal{C}_n^\ell$. The local information is the maximal amount of information one can obtain by measuring any set of operators that cannot be accessed from any smaller-scale subsystem of $\mathcal{C}_n^\ell$ [57,58]. For $\ell > 1$, the local information in subsystem $\mathcal{C}_n^\ell$ is the mutual information of its two largest subsystems, namely $\mathcal{C}_{n-1/2}^{\ell-1}$ and $\mathcal{C}_{n+1/2}^{\ell-1}$, conditioned on their overlap, which is subsystem $\mathcal{C}_n^{\ell-2}$ (see End Matter for details). Formally, the local information i_n^ℓ [57] can be written as

$$i_n^\ell = I(\rho_n^\ell) - I(\rho_{n-1/2}^{\ell-1}) - I(\rho_{n+1/2}^{\ell-1}) + I(\rho_n^{\ell-2}), \quad (1)$$

where $I(\rho_n^\ell) = (\ell+1) - S(\rho_n^\ell)$ is the total information with $S(\rho_n^\ell) = -\mathrm{Tr}[\rho_n^\ell \log_2(\rho_n^\ell)]$ the von Neumann entropy of ρ_n^ℓ, the reduced density matrix of subsystem $\mathcal{C}_n^\ell$. The local information is strictly positive and bounded by two from above, $i_n^\ell \in [0,2]$. The information lattice thereby provides a decomposition of the total information $I(\rho) = \sum_{(n,\ell)} i_n^\ell$ into local information i_n^ℓ.

Stabilizer states are characterized by featuring only integer values of local information, owing to their particular entanglement structure [74,75]. A stabilizer state is the simultaneous $+1$ eigenvector of 2^L Pauli strings, which together form an Abelian group called the stabilizer group. Every stabilizer group is generated by L independent Pauli strings. For a stabilizer state, the operators that yield a maximal amount of information in every subsystem are given by a particular set of stabilizer generators that we call the maximally local generating set [75]. The elements of this set are found at each scale, starting from $\ell = 0$, by selecting the maximum number of independent Pauli strings on that scale belonging to the stabilizer group. This construction continues until there are L independent Pauli strings in the set. The measurement of each of these operators answers a binary question corresponding to one bit of information—namely, whether or not the state is stabilized by the operator. Thus, the local information of every subsystem is an integer.

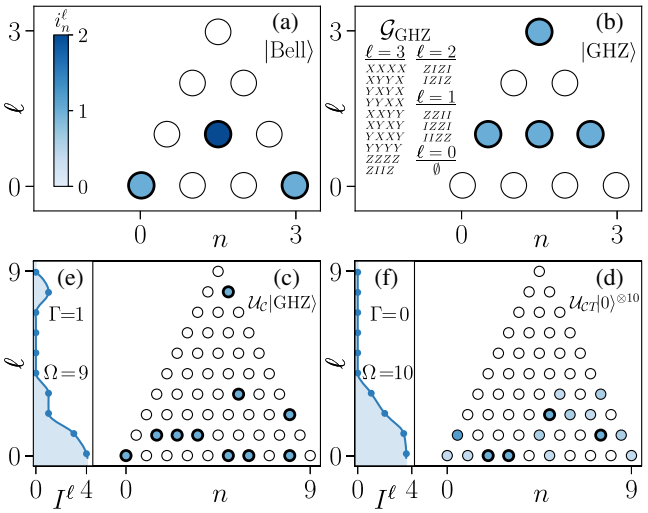


FIG. 1. Information lattice of (a) $|\mathrm{Bell}\rangle = (1/\sqrt{2})(|0101\rangle + |0011\rangle)$, and (b) $|\mathrm{GHZ}\rangle = (1/\sqrt{2})(|0000\rangle + |1111\rangle)$ with its stabilizer group $\mathcal{G}_{\mathrm{GHZ}}$ (excluding the identity operator). (c) Information lattice of a stabilizer state constructed by applying a two-layer random Clifford circuit $\mathcal{U}_{\mathcal{C}}$ to the ten-qubit GHZ state. (d) Information lattice of a short-range nonstabilizer state constructed by applying a random T-doped Clifford circuit $\mathcal{U}_{\mathcal{CT}}$ on the product state $|0\rangle^{\otimes 10}$. The circuit $\mathcal{U}_{\mathcal{CT}}$ is composed of three blocks, each one containing ten layers of Clifford gates and five T gates acting on randomly selected qubits and between two randomly selected Clifford layers. (e),(f) Information per scale I^ℓ of (c) and (d), respectively. In (a)–(d), the color of the sites on the information lattice indicates the amount of local information i_n^ℓ in $\mathcal{C}_n^\ell$, while sites with integer values of i_n^ℓ are circled by bold black lines.

In Fig. 1(a) we show the information lattice of the state $|\mathrm{Bell}\rangle = (1/\sqrt{2})(|0101\rangle + |0011\rangle)$ in which the two center qubits form a Bell pair while each of the two edge qubits is in a product state with the rest. The maximally local generating set for the edge qubits is given by $\{ZIII, -IIIZ\}$. In this case, the measurement of each of these operators answers whether the qubit where the

operator acts nontrivially is in state $|0\rangle$ or $|1\rangle$. The information gained by each of these binary questions is associated with the corresponding site on the information lattice, yielding a local information $i_0^0 = i_3^0 = 1$ fully contained at scale $\ell = 0$. The two bits of information associated with the maximally entangled pair at the center are only accessible by measuring any given pair of two-qubit operators in the set $\{IXXI, IYYI, -IZZI\}$. This is reflected in the information lattice of the state, where $i_1^0 = i_2^0 = 0$ and $i_{1.5}^1 = 2$.

Another example is the four-qubit GHZ state, $|\mathrm{GHZ}\rangle = (1/\sqrt{2})(|0000\rangle + |1111\rangle)$, whose information lattice and stabilizer group are given in Fig. 1(b). The local information of the subsystems at scale $\ell = 1$ is $i_n^1 = 1$ and is associated with the measurement of the stabilizer operators at that scale: $ZZII$, $IZZI$, and $IIZZ$. These operators are independent of each other and belong to the maximally local generating set. At scale $\ell = 2$ there are no stabilizer operators independent from the ones at $\ell = 1$, yielding $i_1^2 = i_3^2 = 0$. The remaining bit of information $i_{1.5}^3 = 1$ is located at the largest scale and can only be accessed by measuring an operator that has nontrivial support on the scale of the entire system. There are ten possible stabilizer operators at the largest scale, and only eight are independent from the stabilizer operators at $\ell = 1$. Choosing one of them, for example $XXXX$, completes a maximally local generating set for the GHZ state. In general, as demonstrated in this and the previous example, the maximally local generating set may not be unique. However, the locality of its operators, dictated by the position of the nonzero local information on the information lattice, is.

For a stabilizer state, the von Neumann information of subsystem $\mathcal{C}_n^\ell$ is given by $I(\rho_n^\ell) = |\mathcal{G}_n^\ell| \leq \ell + 1$, where $|\cdot|$ denotes the rank of a group [74], defined as the number of elements in its generating set (see End Matter for details). $\mathcal{G}_n^\ell$ is the stabilizer subgroup of subsystem $\mathcal{C}_n^\ell$, which contains the elements of the stabilizer group with trivial support in the complement of $\mathcal{C}_n^\ell$. Consequently, the local information in Eq. (1) becomes

$$i_n^\ell = |\mathcal{G}_n^\ell| - |\mathcal{G}_{n-1/2}^{\ell-1}| - |\mathcal{G}_{n+1/2}^{\ell-1}| + |\mathcal{G}_n^{\ell-2}|, \tag{2}$$

which is integer-valued and corresponds to the number of independent generators acting nontrivially only at scale ℓ. This is consistent with the fact that local information is bounded by two from above: increasing a subsystem by one site adds at most two additional independent generators to the maximally local generating set.

Short- and long-range nonstabilizerness via the information lattice—A quantum state has nonstabilizerness if it is not a stabilizer state. Since a stabilizer state necessarily has $i_n^\ell \in \mathbb{N}$, a state with any noninteger value of i_n^ℓ has nonstabilizerness. This is exemplified in Figs. 1(c) and 1(d), where we show the information lattice of a stabilizer state constructed by applying a random Clifford circuit to the ten-qubit GHZ state, and that of a nonstabilizer state constructed by applying a T-doped Clifford circuit to the product state $|0\rangle^{\otimes 10}$. While having noninteger local information is a sufficient condition for a state to have nonstabilizerness, it is not a necessary condition (see End Matter for an example).

We classify nonstabilizerness in terms of its locality by distinguishing short- and long-range nonstabilizer states [71–73]. A state has short-range nonstabilizerness if it can be transformed into a stabilizer state by a shallow local unitary circuit, while a long-range nonstabilizer state requires a local unitary circuit that scales with the system size. To capture these two classes of nonstabilizerness we use the information lattice, which has been shown to classify quantum states in terms of the information per scale,

$$I^\ell = \sum_n i_n^\ell. \tag{3}$$

We are interested in localized states, which exhibit an extensive amount of information per scale at $\ell \ll L$, captured by

$$\Omega = \sum_{\ell=0}^{\lfloor L/2-1 \rfloor} I^\ell. \tag{4}$$

Examples of such states are the ground states of local Hamiltonians and eigenstates of many-body localized systems. Some localized states may also have an intensive $\mathcal{O}(1)$ contribution to local information at scales $\ell \sim L$. This contribution may originate from edge-to-edge correlations, as for example in symmetry-protected topological states, or global correlations, as in cat states [58]. In localized states, the information per scale I^ℓ decays exponentially away from the information peaks both at short and large scales, creating an information gap, see Figs. 1(e) and 1(f). While the information gap is extensive, the $\mathcal{O}(1)$ contribution at large scales stays constant and is captured by the total information at large scales

$$\Gamma = \sum_{\ell=\lfloor L/2 \rfloor}^{L-1} I^\ell, \tag{5}$$

which serves as a universal characteristic of topological phases [58]. In Figs. 1(e) and 1(f) we show the total information per scale of states in Figs. 1(c) and 1(d) and calculate the corresponding values of Γ and Ω.

Under a local unitary circuit the information flow on the information lattice is strictly local. As a result the only way to close the information gap and redistribute information between Ω and Γ is by applying a circuit that scales with the system size. For an information gap extending over g scales, the minimum depth of such a circuit is roughly $g/4$, thus $\sim\mathcal{O}(L)$ [57,63]. Consequently, a localized state with

noninteger Γ cannot be transformed into a stabilizer state, which always has integer Γ, by any shallow local unitary circuit. Thus, $\Gamma \notin \mathbb{N}$ is a witness of long-range nonstabilizerness for localized states. This implies that a localized state with $\Gamma = 0$ can have at most short-range nonstabilizerness, as for example is the case for the state in Fig. 1(d).

In localized states in the thermodynamic limit, the total information at large scales Γ separates into contributions coming from edge-to-edge and global correlations, such that $\Gamma =: \gamma_{\text{edge}} + \gamma_{\text{global}}$. To estimate γ_{global} in a given state, we employ a folding procedure in which sites n and $L - n - 1$ are combined, reducing the chain length by half, while doubling the local Hilbert space dimension at each site. Because of this coarse graining, the edge-to-edge correlations of the initial chain become local on the information lattice of the folded chain. Therefore, only the global correlations survive at large scales and the total information at large scales of the folded information lattice Γ_{folded}, calculated according to Eq. (5) with $L \to L' = L/2$, provides an estimate of γ_{global} (see End Matter). In the next section, we show that the symmetric ground state of the spin-1/2 three-state Potts model realizes long-range nonstabilizerness.

Spin-1/2 three-state Potts model—The three-state Potts model [76] is described by the Hamiltonian

$$H = -\frac{J}{3}\sum_{i}^{N-1}(Z_i^\dagger Z_{i+1} + Z_{i+1}^\dagger Z_i) - h\sum_{i}^{N}(X_i^\dagger + X_i), \tag{6}$$

$$Z_i = \begin{pmatrix} 1 & 0 & 0 \\ 0 & \omega & 0 \\ 0 & 0 & \omega^2 \end{pmatrix}, \quad X_i = \begin{pmatrix} 0 & 0 & 1 \\ 1 & 0 & 0 \\ 0 & 1 & 0 \end{pmatrix}, \tag{7}$$

with $J, h \geq 0$ the interaction strength and the transverse magnetic field, respectively, and $\omega = e^{2\pi i/3}$. This model has a $\mathbb{Z}_3$ rotational symmetry realized by $\prod_{i=1}^{N} X_i$, and undergoes a phase transition at the self-dual point $J/3 = h$ between a symmetry-broken phase with a threefold degenerate ground state and a paramagnetic phase with a unique ground state [77]. We realize this model in a spin-1/2 chain of length $L = 2N$ by projecting each pair of neighboring spins onto the triplet subspace, onto which the operators Z_i and X_i act.

We characterize the nonstabilizerness in the symmetric ground state for different values of h and L at fixed $J = 1$. The information lattice of the symmetric ground state for $h \ll 1/3$ is shown in the right inset of Fig. 2 with $h = 0$ and $L = 12$. There is an extensive amount of information at small scales $\Omega \sim \mathcal{O}(L)$ and a finite contribution at large scales Γ separated by an information gap. The same features are also clearly visible in the information per scale as shown in the left inset of Fig. 2. The noninteger $\Gamma \approx \log_2(3)$ in the presence of an information gap indicates the long-range nonstabilizerness of the state (see End Matter for further details on this value of Γ). For $h \gg 1/3$ the value of Γ goes to zero, and local information is present at small scales only, which indicates at most short-range nonstabilizerness. In Fig. 2 we show both Γ and Γ_{folded} as functions of h for different system sizes L, where curves for different L cross approximately at the phase transition point $h = 1/3$. There is a systematic flow on both sides of the crossings such that Γ and Γ_{folded} approach either $\log_2(3)$ or 0 as L increases. Away from the critical point, for $h \lesssim 0.2$, the total information at large scales for the folded information lattice is $\Gamma_{\text{folded}} \approx \Gamma$, which indicates that long-range nonstabilizerness originates from global correlations. In the vicinity of the critical point, the information gap closes and nonzero local information is present at all scales. Thus Γ scales with system size and is no longer a witness of long-range nonstabilizerness. In this case, the folding procedure rearranges local information on the folded information lattice such that there are additional contributions at large scales making Γ_{folded} overestimate the global correlations γ_{global}.

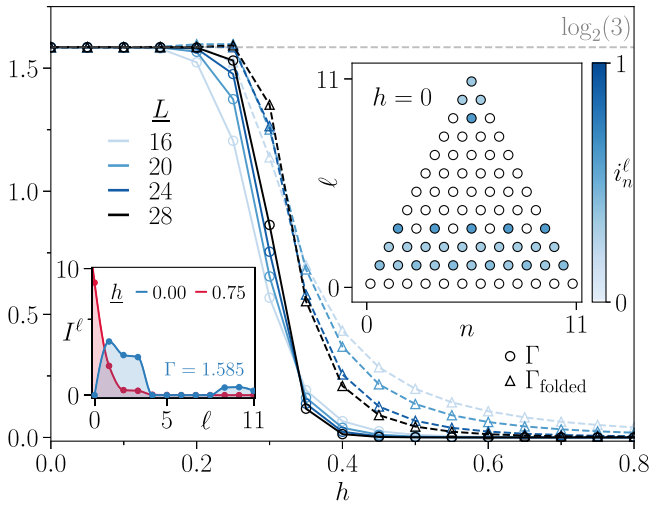


FIG. 2. The total information at large scales in the unfolded and folded chain of the symmetric ground state of the spin-1/2 three-state Potts model, as a function of the magnetic field h and system size L, with $J = 1$. The inset on the right shows the information lattice of the symmetric ground state at $h = 0$ and $L = 12$. The left inset shows the information per scale for the same state (blue line) and for the paramagnetic ground state at $h = 0.75$ and $L = 12$ (red line).

Discussion—We have shown that the information lattice provides a straightforward and direct way to identify nonstabilizerness in any quantum state. This stems from the fact that local information in a stabilizer state is necessarily an integer. In localized states, defined by the presence of an information gap, the information lattice allows us to detect long-range nonstabilizerness. The information gap prevents the redistribution of information between short and large scales under shallow local unitary circuits, making the total information at large scales Γ an

invariant. As a consequence, a noninteger Γ serves as a witness of long-range nonstabilizerness, since it indicates that a state cannot be transformed into a stabilizer state by any shallow local unitary circuit. Using a folding procedure we further identify global and edge-to-edge contributions to Γ. Our method directly witnesses long-range nonstabilizerness without the need of employing any minimization procedure or a search for a shallow local unitary circuit connecting the state to a stabilizer state.

As an example we have analyzed the long-range nonstabilizerness of the spin-$1/2$ three-state Potts model. At small magnetic field the symmetric ground state of the model has large-scale information $\Gamma \approx \log_2(3)$, indicating long-range nonstabilizerness. This comes directly from the fact that the ground state is threefold degenerate. For a large magnetic field, $\Gamma \approx 0$ indicates at most short-range nonstabilizerness. At the phase transition between these two limits the ground state is no longer localized as the information gap closes and Γ cannot be used as a witness of long-range nonstabilizerness.

Since the information lattice is a state property, our approach is independent of any parent Hamiltonian or any protocol used to generate quantum states and aids in the current efforts to characterize states in terms of the scale of their nonstabilizerness. Witnessing long-range nonstabilizerness from Γ in localized states is computationally efficient [58,78] as compared to brute-force methods involving minimization of nonstabilizerness monotones over all possible local unitary circuits (see End Matter). The properties discussed in this Letter are also potentially accessible through experiments as the density matrix can be reconstructed experimentally through quantum state tomography [79–83].

While in this Letter we focused on one-dimensional systems, a possible future direction is to study nonstabilizerness in localized states in higher dimensions. Our framework can be readily used via a quasi-1D approach, in which the information lattice of an effective one-dimensional system is obtained by coarse-graining a higher-dimensional system. More generally, one could explore long-range nonstabilizerness in higher dimensions via a higher-dimensional local decomposition of information [84]. Another direction is to explore nonstabilizerness in mixed-state phases [85,86], to which the information lattice is directly applicable. Furthermore, generalizing the characterization of quantum states by the scale of their nonstabilizerness requires constructing a fully local decomposition of nonstabilizerness akin to the information lattice. This is, for example, relevant for characterizing critical and ergodic states.

Acknowledgments—We thank D. Aceituno Chávez, I. M. Flór and A. Partos for useful discussions. This work received funding from the European Research Council (ERC) under the European Union's Horizon 2020 research and innovation program (Grant Agreement No. 101001902), the Swedish Research Council (VR) through Grant No. 2020-00214, and the Knut and Alice Wallenberg Foundation (KAW) via the project Dynamic Quantum Matter (No. 2019.0068). T. K. K. acknowledges funding from the Wenner-Gren Foundations. The computations were enabled by resources provided by the National Academic Infrastructure for Supercomputing in Sweden (NAISS), partially funded by the Swedish Research Council through Grant Agreement No. 2022-06725.

Data availability—The data that support the findings of this article are openly available [87].

[1] M. Srednicki, Entropy and area, Phys. Rev. Lett. **71**, 666 (1993).
[2] M. B. Hastings, An area law for one-dimensional quantum systems, J. Stat. Mech. (2007) P08024.
[3] M. M. Wolf, F. Verstraete, M. B. Hastings, and J. I. Cirac, Area laws in quantum systems: Mutual information and correlations, Phys. Rev. Lett. **100**, 070502 (2008).
[4] J. Eisert, M. Cramer, and M. B. Plenio, Colloquium: Area laws for the entanglement entropy, Rev. Mod. Phys. **82**, 277 (2010).
[5] J. M. Deutsch, Quantum statistical mechanics in a closed system, Phys. Rev. A **43**, 2046 (1991).
[6] M. Srednicki, Chaos and quantum thermalization, Phys. Rev. E **50**, 888 (1994).
[7] M. Rigol, V. Dunjko, and M. Olshanii, Thermalization and its mechanism for generic isolated quantum systems, Nature (London) **452**, 854 (2008).
[8] N. Laflorencie, Quantum entanglement in condensed matter systems, Phys. Rep. **646**, 1 (2016).
[9] B. Zeng, X. Chen, D.-L. Zhou, X.-G. Wen *et al.*, *Quantum Information Meets Quantum Matter* (Springer, New York, 2019).
[10] U. Schollwöck, The density-matrix renormalization group in the age of matrix product states, Ann. Phys. (Amsterdam) **326**, 96 (2011).
[11] J. I. Cirac, D. Pérez-García, N. Schuch, and F. Verstraete, Matrix product states and projected entangled pair states: Concepts, symmetries, theorems, Rev. Mod. Phys. **93**, 045003 (2021).
[12] A. Hamma, R. Ionicioiu, and P. Zanardi, Ground state entanglement and geometric entropy in the Kitaev model, Phys. Lett. A **337**, 22 (2005).
[13] A. Kitaev and J. Preskill, Topological entanglement entropy, Phys. Rev. Lett. **96**, 110404 (2006).
[14] M. Levin and X.-G. Wen, Detecting topological order in a ground state wave function, Phys. Rev. Lett. **96**, 110405 (2006).
[15] X. Chen, Z.-C. Gu, and X.-G. Wen, Local unitary transformation, long-range quantum entanglement, wave function renormalization, and topological order, Phys. Rev. B **82**, 155138 (2010).
[16] S. Mas-Mendoza, R. D. P. East, M. Filippone, and A. G. Grushin, A graphical diagnostic of topological order using ZX calculus, arXiv:2509.12355.

[17] E. Knill, Non-binary unitary error bases and quantum codes, arXiv:quant-ph/9608048.
[18] D. Gottesman, The Heisenberg representation of quantum computers, arXiv:quant-ph/9807006.
[19] J. Emerson, D. Gottesman, S. A. H. Mousavian, and V. Veitch, The resource theory of stabilizer quantum computation, New J. Phys. **16**, 013009 (2014).
[20] M. Howard and E. Campbell, Application of a resource theory for magic states to fault-tolerant quantum computing, Phys. Rev. Lett. **118**, 090501 (2017).
[21] S. Bravyi, D. Browne, P. Calpin, E. Campbell, D. Gosset, and M. Howard, Simulation of quantum circuits by low-rank stabilizer decompositions, Quantum **3**, 181 (2019).
[22] L. Leone, Salvatore F. E. Oliviero, and A. Hamma, Stabilizer Rényi entropy, Phys. Rev. Lett. **128**, 050402 (2022).
[23] J. Jiang and X. Wang, Lower bound for the T count via unitary stabilizer nullity, Phys. Rev. Appl. **19**, 034052 (2023).
[24] E. Tirrito, P. S. Tarabunga, G. Lami, T. Chanda, L. Leone, Salvatore F. E. Oliviero, M. Dalmonte, M. Collura, and A. Hamma, Quantifying nonstabilizerness through entanglement spectrum flatness, Phys. Rev. A **109**, L040401 (2024).
[25] N. Dowling, P. Kos, and X. Turkeshi, Magic resources of the Heisenberg picture, Phys. Rev. Lett. **135**, 050401 (2025).
[26] N. Dowling, K. Modi, and Gregory A. L. White, Bridging entanglement and magic resources within operator space, Phys. Rev. Lett. **135**, 160201 (2025).
[27] A. Paviglianiti, G. Lami, M. Collura, and A. Silva, Estimating nonstabilizerness dynamics without simulating it, PRX Quantum **6**, 030320 (2025).
[28] D. Gottesman, Stabilizer codes and quantum error correction, arXiv:quant-ph/9705052.
[29] D. Gottesman, Theory of fault-tolerant quantum computation, Phys. Rev. A **57**, 127 (1998).
[30] S. Bravyi and A. Kitaev, Universal quantum computation with ideal Clifford gates and noisy ancillas, Phys. Rev. A **71**, 022316 (2005).
[31] A. G. Fowler, M. Mariantoni, J. M. Martinis, and A. N. Cleland, Surface codes: Towards practical large-scale quantum computation, Phys. Rev. A **86**, 032324 (2012).
[32] S. Sarkar, C. Mukhopadhyay, and A. Bayat, Characterization of an operational quantum resource in a critical many-body system, New J. Phys. **22**, 083077 (2020).
[33] Salvatore F. E. Oliviero, L. Leone, and A. Hamma, Magic-state resource theory for the ground state of the transverse-field Ising model, Phys. Rev. A **106**, 042426 (2022).
[34] D. Rattacaso, L. Leone, Salvatore F. E. Oliviero, and A. Hamma, Stabilizer entropy dynamics after a quantum quench, Phys. Rev. A **108**, 042407 (2023).
[35] G. Passarelli, R. Fazio, and P. Lucignano, Nonstabilizerness of permutationally invariant systems, Phys. Rev. A **110**, 022436 (2024).
[36] P. S. Tarabunga, Critical behaviors of non-stabilizerness in quantum spin chains, Quantum **8**, 1413 (2024).
[37] M. Bejan, C. McLauchlan, and B. Béri, Dynamical Magic Transitions in Monitored Clifford + T Circuits, PRX Quantum **5**, 030332 (2024).
[38] G. E. Fux, B. Béri, R. Fazio, and E. Tirrito, Disentangling unitary dynamics with classically simulable quantum circuits, Phys. Rev. Lett. **135**, 260605 (2025).
[39] X. Turkeshi, A. Dymarsky, and P. Sierant, Pauli spectrum and nonstabilizerness of typical quantum many-body states, Phys. Rev. B **111**, 054301 (2025).
[40] G. Passarelli, P. Lucignano, D. Rossini, and A. Russomanno, Chaos and magic in the dissipative quantum kicked top, Quantum **9**, 1653 (2025).
[41] E. Tirrito, X. Turkeshi, and P. Sierant, Anticoncentration and nonstabilizerness spreading under ergodic quantum dynamics, arXiv:2412.10229.
[42] E. Tirrito, L. Lumia, A. Paviglianiti, G. Lami, A. Silva, X. Turkeshi, and M. Collura, Magic phase transitions in monitored gaussian fermions, arXiv:2507.07179.
[43] A. Russomanno, G. Passarelli, D. Rossini, and P. Lucignano, Nonstabilizerness in the unitary and monitored quantum dynamics of XXZ-staggered and Sachdev-Ye-Kitaev models, Phys. Rev. B **112**, 064312 (2025).
[44] J. Odavić, M. Viscardi, and A. Hamma, Stabilizer entropy in nonintegrable quantum evolutions, Phys. Rev. B **112**, 104301 (2025).
[45] M. Viscardi, M. Dalmonte, A. Hamma, and E. Tirrito, Interplay of entanglement structures and stabilizer entropy in spin models, SciPost Phys. Core **9**, 012 (2026).
[46] M. Collura, J. D. Nardis, V. Alba, and G. Lami, The nonstabilizerness of fermionic Gaussian states, Quantum **10**, 2036 (2026).
[47] M. Sarkis and A. Tkatchenko, Are molecules magical? Non-Stabilizerness in molecular bonding, arXiv:2504.06673.
[48] X. Turkeshi, E. Tirrito, and P. Sierant, Magic spreading in random quantum circuits, Nat. Commun. **16**, 2575 (2025).
[49] P. R. N. Falcão, P. Sierant, J. Zakrzewski, and E. Tirrito, Magic dynamics in many-body localized systems, Phys. Rev. Lett. **135**, 240404 (2025).
[50] T. Hernández-Yanes, P. Sierant, J. Zakrzewski, and M. Płodzień, Non-stabilizerness in quantum-enhanced metrological protocols, Phys. Rev. A **113**, 012416 (2026).
[51] G. C. Santra, A. Windey, S. Bandyopadhyay, A. Legramandi, and P. Hauke, Complexity transitions in chaotic quantum systems: Nonstabilizerness, entanglement, and fractal dimension in SYK and random matrix models, arXiv:2505.09707.
[52] T. Haug, L. Aolita, and M. Kim, Probing quantum complexity via universal saturation of stabilizer entropies, Quantum **9**, 1801 (2025).
[53] P. Sierant, P. Stornati, and X. Turkeshi, Fermionic magic resources of quantum many-body systems, PRX Quantum **7**, 010302 (2026).
[54] J. Huang, X. Qian, and M. Qin, Nonstabilizerness entanglement entropy: A measure of hardness in the classical simulation of quantum many-body systems with tensor network states, Phys. Rev. A **112**, 012425 (2025).
[55] L. G. Valiant, Quantum computers that can be simulated classically in polynomial time, in *Proceedings of the Thirty-Third Annual ACM Symposium on Theory of Computing*, STOC '01 (Association for Computing Machinery, New York, NY, USA, 2001), pp. 114–123.
[56] B. M. Terhal and D. P. DiVincenzo, Classical simulation of noninteracting-fermion quantum circuits, Phys. Rev. A **65**, 032325 (2002).
[57] T. Klein Kvorning, L. Herviou, and J. H. Bardarson, Time-evolution of local information: Thermalization dynamics of local observables, SciPost Phys. **13**, 080 (2022).

[58] C. Artiaco, T. Klein Kvorning, D. Aceituno Chávez, L. Herviou, and J. H. Bardarson, Universal characterization of quantum many-body states through local information, Phys. Rev. Lett. **134**, 190401 (2025).
[59] N. P. Bauer, B. Trauzettel, T. Klein Kvorning, J. H. Bardarson, and C. Artiaco, Local information flow in quantum quench dynamics, Phys. Rev. A **112**, 022221 (2025).
[60] C. Artiaco, J. Barata, and E. Rico, Out-of-equilibrium dynamics in a U(1) lattice gauge theory via local information flows: Scattering and string breaking, arXiv:2510.16101 (2025).
[61] J. Barata, J. Hormaza, Z.-B. Kang, and W. Qian, Hadronic scattering in $(1+1)$D SU(2) lattice gauge theory from tensor networks, J. High Energy Phys. 06 (2026) 168.
[62] A. Nava, C. Artiaco, Y. Gefen, I. Gornyi, M. Tsitsishvili, A. Zazunov, and R. Egger, Information transport and transport-induced entanglement in open fermion chains, Phys. Rev. Res. **8**, 033273 (2026).
[63] C. Artiaco, C. Fleckenstein, D. Aceituno Chávez, T. K. Kvorning, and J. H. Bardarson, Efficient large-scale many-body quantum dynamics via local-information time evolution, PRX Quantum **5**, 020352 (2024).
[64] K. Harkins, C. Fleckenstein, N. D'Souza, P. M. Schindler, D. Marchiori, C. Artiaco, Q. Reynard-Feytis, U. Basumallick, W. Beatrez, A. Pillai, M. Hagn, A. Nayak, S. Breuer, X. Lv, M. McAllister, P. Reshetikhin, E. Druga, M. Bukov, and A. Ajoy, Nanoscale engineering and dynamic stabilization of mesoscopic spin textures, Sci. Adv. **11**, eadn9021 (2025).
[65] P. S. Tarabunga, E. Tirrito, T. Chanda, and M. Dalmonte, Many-body magic via Pauli-Markov chains—from criticality to gauge theories, PRX Quantum **4**, 040317 (2023).
[66] D. Qian and J. Wang, Quantum nonlocal nonstabilizerness, Phys. Rev. A **111**, 052443 (2025).
[67] C. Cao, Non-trivial area operators require non-local magic, J. High Energy Phys. 11 (2024) 105.
[68] C. J. Cao, G. Cheng, A. Hamma, L. Leone, W. Munizzi, and Savatore F. Oliviero, Gravitational backreaction is magical, PRX Quantum **6**, 040375 (2025).
[69] P. S. Tarabunga and T. Haug, Efficient mutual magic and magic capacity with matrix product states, SciPost Phys. **19**, 085 (2025).
[70] H. Timsina, Y.-M. Ding, E. Tirrito, P. S. Tarabunga, B.-B. Mao, M. Collura, Z. Yan, and M. Dalmonte, Robustness of Magic in the quantum Ising chain via Quantum Monte Carlo tomography, Phys. Rev. B **112**, 165135 (2025).
[71] C. D. White, C. J. Cao, and B. Swingle, Conformal field theories are magical, Phys. Rev. B **103**, 075145 (2021).
[72] T. D. Ellison, K. Kato, Z.-W. Liu, and T. H. Hsieh, Symmetry-protected sign problem and magic in quantum phases of matter, Quantum **5**, 612 (2021).
[73] D. A. Korbany, M. J. Gullans, and L. Piroli, Long-range nonstabilizerness and phases of matter, Phys. Rev. Lett. **135**, 160404 (2025).
[74] D. Fattal, T. S. Cubitt, Y. Yamamoto, S. Bravyi, and I. L. Chuang, Entanglement in the stabilizer formalism, arXiv:quant-ph/0406168.
[75] V. Sharma and E. J. Mueller, Multipartite entanglement structures in quantum stabilizer states, Phys. Rev. A **112**, 012411 (2025).
[76] F. Y. Wu, The Potts model, Rev. Mod. Phys. **54**, 235 (1982).
[77] R. S. K. Mong, D. J. Clarke, J. Alicea, N. H. Lindner, and P. Fendley, Parafermionic conformal field theory on the lattice, J. Phys. A **47**, 452001 (2014).
[78] D. Aceituno Chávez, Thermalization and localization: Novel perspectives from random circuits and the information lattice (Ph.D. Thesis), 2024.
[79] D. T. Smithey, M. Beck, M. G. Raymer, and A. Faridani, Measurement of the wigner distribution and the density matrix of a light mode using optical homodyne tomography: Application to squeezed states and the vacuum, Phys. Rev. Lett. **70**, 1244 (1993).
[80] U. Leonhardt, Quantum-state tomography and discrete Wigner function, Phys. Rev. Lett. **74**, 4101 (1995).
[81] D. Leibfried, D. M. Meekhof, B. E. King, C. Monroe, W. M. Itano, and D. J. Wineland, Experimental determination of the motional quantum state of a trapped atom, Phys. Rev. Lett. **77**, 4281 (1996).
[82] A. I. Lvovsky and M. G. Raymer, Continuous-variable optical quantum-state tomography, Rev. Mod. Phys. **81**, 299 (2009).
[83] M. Cramer, M. B. Plenio, S. T. Flammia, R. Somma, D. Gross, S. D. Bartlett, O. Landon-Cardinal, D. Poulin, and Y.-K. Liu, Efficient quantum state tomography, Nat. Commun. **1**, 149 (2010).
[84] I. M. Flór, C. Artiaco, T. K. Kvorning, and J. H. Bardarson, Higher-dimensional information lattice: Quantum state characterization through inclusion-exclusion local information, arXiv:2512.20793.
[85] S. Sang, Y. Zou, and T. H. Hsieh, Mixed-state quantum phases: Renormalization and quantum error correction, Phys. Rev. X **14**, 031044 (2024).
[86] S. Sang, L. A. Lessa, R. S. K. Mong, T. Grover, C. Wang, and T. H. Hsieh, Mixed-state phases from local reversibility, arXiv:2507.02292.
[87] Y. Bilinskaya, M. F. Martínez, S. Ghosh, T. Klein Kvorning, C. Artiaco, and J. H. Bardarson, Witnessing short- and long-range nonstabilizerness via the information lattice, 10.5281/zenodo.17608434 (2025).

End Matter

Interpretation of local information in terms of conditional mutual information—The local information i_n^ℓ [57] at position (n,ℓ) associated with the subsystem $\mathcal{C}_n^\ell$ is the mutual information shared by the largest lower-scale subsystems $\mathcal{C}_{n-1/2}^{\ell-1}$ and $\mathcal{C}_{n+1/2}^{\ell-1}$ (consisting of sites $[0,\ell-1]$ and $[1,\ell]$, respectively) conditioned on the total information available in their overlap, namely the subsystem $\mathcal{C}_n^{\ell-2}$ consisting of sites $[1,\ell-1]$. For example, $i_{4.5}^5$ is the mutual information between subsystems $\mathcal{C}_4^4$ containing the sites [2,6] and $\mathcal{C}_5^4$ containing the

sites [3,7], conditioned on their overlap, which is the subsystem $\mathcal{C}^3_{4.5}$ containing sites [3,6].

At scale $\ell = 0$ all subsystems are single-qubit, such that the local information is simply the von Neumann information

$$i^0_n \coloneqq I(\mathcal{C}^0_n). \tag{A1}$$

At scale $\ell = 1$ the subsystems are two-qubit and can only be partitioned into two single-qubit nonoverlapping subsystems $\mathcal{C}^0_{n-1/2}$ and $\mathcal{C}^0_{n+1/2}$ for any n. The local information at any $(n, \ell = 1)$ is thus equivalent to mutual information of the lower scale subsystems in the absence of overlapping regions and is given by

$$\begin{aligned} i^1_n &\coloneqq i(\mathcal{C}^0_{n-1/2}; \mathcal{C}^0_{n+1/2}) \\ &= I(\rho^1_n) - I(\rho^0_{n-1/2}) - I(\rho^0_{n+1/2}). \end{aligned} \tag{A2}$$

At scale $\ell = 2$, all subsystems $\mathcal{C}^2_n$ consist of three qubits and the largest lower scale subsystems contained within them are $\mathcal{C}^1_{n-1/2}, \mathcal{C}^1_{n+1/2}$, each consisting of two qubits, such that they overlap at subsystem $\mathcal{C}^0_n$. The local information at any $(n, \ell = 2)$ is thus the mutual information of the lower-scale two qubit subsystems conditioned on the information available to the single-qubit overlap $\mathcal{C}^0_n$ and is given by

$$\begin{aligned} i^2_n &\coloneqq i(\mathcal{C}^1_{n-1/2}; \mathcal{C}^1_{n+1/2} | \mathcal{C}^0_n) \\ &= I(\rho^2_n) - I(\rho^1_{n-1/2}) - I(\rho^1_{n+1/2}) + I(\rho^0_n). \end{aligned} \tag{A3}$$

For any $\ell > 2$ the definition is the same as in Eq. (A3), where the overlap contains $\ell - 1$ sites, thus

$$i^\ell_n \coloneqq \begin{cases} I(\mathcal{C}^\ell_n), & \ell = 0 \\ I(\mathcal{C}^{\ell-1}_{n-1/2}; \mathcal{C}^{\ell-1}_{n+1/2} | \mathcal{C}^{\ell-2}_n), & \ell > 1. \end{cases} \tag{A4}$$

Written in terms of disjoint subsystems, this definition is equivalent to the conditional mutual information of the leftmost qubit $\mathcal{C}^0_{n-\ell/2}$ and the rightmost qubit $\mathcal{C}^0_{n+\ell/2}$ conditioned on the intermediate region $\mathcal{C}^{\ell-2}_n$, such that $i^\ell_n = I(\mathcal{C}^0_{n-\ell/2}; \mathcal{C}^0_{n+\ell/2} | \mathcal{C}^{\ell-2}_n)$.

Von Neumann entropy of stabilizer states—Following Ref. [74], the density matrix of an L-qubit stabilizer state $|\psi\rangle = |0\rangle^{\otimes L}$, where $\mathcal{U}_\mathcal{C}$ is a Clifford circuit, can be written in the form

$$\begin{aligned} \rho = |\psi\rangle\langle\psi| &= \mathcal{U}_\mathcal{C} |0\rangle^{\otimes L} \langle 0|^{\otimes L} \mathcal{U}_\mathcal{C}^\dagger \\ &= \mathcal{U}_\mathcal{C} \prod_i^L \frac{\mathbb{I} + Z_i}{2} \mathcal{U}_\mathcal{C}^\dagger = \frac{1}{2^L} \prod_i^L (\mathbb{I} + g_i) = \frac{1}{2^L} \sum_{g \in \mathcal{G}} g, \end{aligned} \tag{B1}$$

where $\mathbb{I}$ is the identity matrix, g are the elements of the stabilizer group $\mathcal{G}$ of the state, and g_i are the generators. Decomposing the chain into two disjoint subsystems, A and B, the reduced density matrix of subsystem A can be written as

$$\begin{aligned} \rho_A = \mathrm{Tr}_B(\rho) &= \mathrm{Tr}_B \left(\frac{1}{2^L} \sum_{g \in \mathcal{G}} g \right) = \frac{1}{2^L} \sum_{g \in \mathcal{G}} \mathrm{Tr}(g_B) g_A \\ &= \frac{2^{L_B}}{2^L} \sum_{g_A \in \mathcal{G}_A} g_A = \frac{1}{2^{L_A}} \sum_{g_A \in \mathcal{G}_A} g_A, \end{aligned} \tag{B2}$$

where $\mathcal{G}_A$ is the stabilizer subgroup for subsystem A, $L = L_A + L_B$, and we used the fact that the trace of any Pauli matrix vanishes except in the case of identity, which gives 2^N. The von Neumann entropy of subsystem A can be calculated using that

$$\begin{aligned} \rho^2_A &= \frac{1}{2^{L_A}} \frac{1}{2^{L_A}} \sum_{g_A \in \mathcal{G}_A} \sum_{\tilde{g}_A \in \mathcal{G}_A} g_A \tilde{g}_A \\ &= \frac{1}{2^{L_A}} \sum_{\tilde{g}_A \in \mathcal{G}_A} \left(\frac{1}{2^{L_A}} \sum_{g'_A \in \mathcal{G}_A} g'_A \right) = \frac{\dim(\mathcal{G}_A)}{2^{L_A}} \rho_A. \end{aligned} \tag{B3}$$

This means that the nonzero eigenvalues of the reduced density matrix of a stabilizer state are completely degenerate and equal to $\lambda = \dim(\mathcal{G}_A)/2^{L_A}$, and since ρ_A has unit trace there are exactly $2^{N_A}/\dim(\mathcal{G}_A)$ such nonzero eigenvalues. The von Neumann entropy of a subsystem is then given by

$$\begin{aligned} S(\rho_A) &= -\mathrm{Tr}\{\rho_A \log \rho_A\} = -\sum_\lambda \lambda \log \lambda \\ &= -\frac{2^{L_A}}{\dim(\mathcal{G}_A)} \frac{\dim(\mathcal{G}_A)}{2^{L_A}} \log \left(\frac{\dim(\mathcal{G}_A)}{2^{L_A}} \right) = L_A - |\mathcal{G}_A|, \end{aligned} \tag{B4}$$

where $|\mathcal{G}|$ is the rank of the stabilizer subgroup.

Fine-tuned example of a nonstabilizer state with integer values of local information—A four-qubit state with only integer local values on the information lattice is given by $|\Psi\rangle = \sum_{k=1}^4 \sqrt{\lambda_k} |B_k\rangle_{12} \mathrm{CZ}_{34} |B_k\rangle_{34}$, with $|B_k\rangle$ the four Bell-pair states, CZ_{34} a controlled Z gate between the third and fourth qubits, and values of λ_k given by (0.097 921 646 2, 0.097 921 646 2, 0.012 106 218 3, 0.792 050 489 4). These integer values of the local information are not robust under random Clifford evolution, indicating that the state $|\Psi\rangle$ is a nonstabilizer state.

The folding procedure—The folding procedure is shown in Fig. 3(a), where the chain of length $L = 6$ is folded across the gray dashed line at its middle point, resulting in a folded chain of length $L' = 3$. The sites in the folded chain are given by the blue ovals, denoted by n', and encompass those sites of the unfolded chain, n,

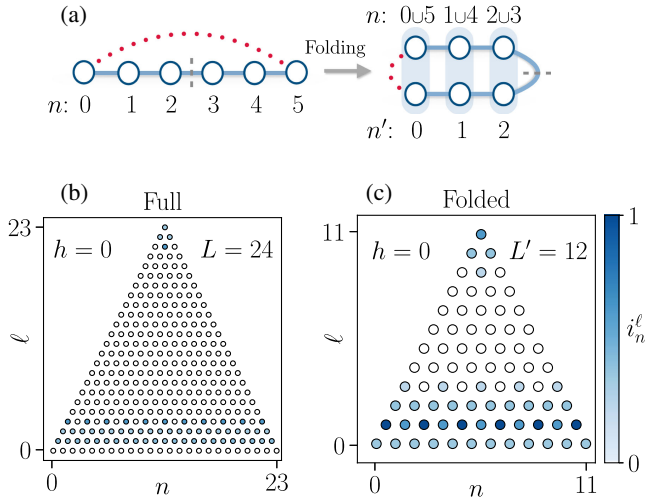


FIG. 3. (a) Sketch of the folding procedure used to estimate γ_{global} in a chain of length $L = 6$. (b) Information lattice of the symmetric ground state of the spin-1/2 three-state Potts model at $h = 0$ and for system size $L = 24$. (c) Folded information lattice for (b).

belonging to each oval. The dotted red line sketches an edge-to-edge correlation between sites $n = 0$ and $n = 5$ in the unfolded chain, which becomes completely local to site $n' = 0$ in the folded chain. Global correlations, on the other hand, do not become local upon folding, and their sum at large scales is unchanged. An example of the information lattice calculated for the symmetric ground of the of the spin-1/2 three-state Potts model from the main text at $h = 0$ and $L = 24$ is shown in Fig. 3(b), while its folded counterpart is shown in 3(c).

Γ *in symmetry broken states*—Long-range nonstabilizerness may arise in quantum systems when the ground state of the Hamiltonian is degenerate. This occurs, for example, when there is a spontaneously broken symmetry. In the symmetric ground state, $\log_2(q)$ bits of information are associated with the relative phases between the different q degenerate states breaking the symmetry. This results in $\Gamma = \log_2(q)$, thus $q \neq 2^x$ with $x \in \mathbb{N}$ implies $\Gamma \notin \mathbb{N}$ and long-range nonstabilizerness. If the degenerate states are product states, the bipartite entanglement entropy $S = \log_2(q)$ across any cut and thus equals Γ. This is, however, not generic, and S does not suffice to extract Γ.

Computational cost—The cost of calculating the information lattice for a generic state scales exponentially with L, the limiting factor being the diagonalization of the density matrices at the scale $\ell \sim L/2$. In a localized state the nonzero local information resides only at the small and large scales, which can be efficiently calculated [58,78]. This is due to the fact that for a pure state the entanglement entropy of the reduced density matrix is equal to that of its complement. Thus, witnessing long-range nonstabilizerness via Γ is computationally less expensive than minimizing a nonstabilizerness monotone over all possible local unitary circuits.